



STRUCTURAL SCIENCE  
CRYSTAL ENGINEERING  
MATERIALS

Volume 73 (2017)

**Supporting information for article:**

**Exploring charge density analysis in crystals at high pressure; data collection, data analysis and advanced modelling**

**Nicola Casati, Alessandro Genoni, Benjamin Meyer, Anna Krawczuk and Piero Macchi**

**Table S1** Selected crystallographic data and spherical atom refinement parameters for the low temperature data collections. The space group P2<sub>1</sub>/n remains unchanged during the cooling. Resolution is 0.67 Å for all datasets.

T (K)	90	123	183	243	298
a (Å)	9.0425(1)	9.0481(1)	9.6081(1)	9.0759(1)	9.0915(1)
b (Å)	12.6672(1)	12.6786(1)	12.7038(1)	12.7323(1)	12.7606(1)
c (Å)	9.6675(1)	9.6881(1)	9.7292(1)	9.7769(1)	9.8227(1)
β (°)	94.337(1)	94.415(1)	94.501(1)	94.607(1)	94.706(1)
V (Å <sup>3</sup> )	1104.11(2)	1108.10(2)	1116.45(2)	1126.14(2)	1135.72(2)
Reflections:					
Total/unique	13844/3582	14231/3594	14324/3620	14464/3650	14579/3686
R <sub>int</sub>	0.0252	0.0254	0.0263	0.0286	0.0285
R <sub>1</sub>	0.0372	0.0371	0.0384	0.0399	0.0408
Δρ min/max (eÅ <sup>-3</sup> )	-0.24/0.39	-0.22/0.38	-0.21/0.32	-0.19/0.28	-0.16/0.23

**Table S2** Bond distances from the refined models of the high pressure experiments

P(GPa)	1.8	4.35	5.8	7.7 <sup>1</sup>	7.95	9.5
C1 - C14	1.383(5)	1.379(4)	1.374(4)	1.376(2)	1.368(4)	1.362(5)
C1 - C2	1.408(5)	1.412(5)	1.411(4)	1.414(2)	1.412(4)	1.418(5)
C2 - C3	1.366(6)	1.374(5)	1.359(5)	1.373(2)	1.359(4)	1.359(6)
C3 - C4	1.417(6)	1.411(5)	1.422(5)	1.429(3)	1.430(5)	1.428(6)
C4 - C5	1.376(6)	1.370(5)	1.372(4)	1.374(3)	1.367(4)	1.362(5)
C5 - C6	1.393(5)	1.413(5)	1.403(4)	1.413(2)	1.411(4)	1.404(6)
C6 - C7	1.400(5)	1.385(4)	1.388(4)	1.381(4)	1.376(4)	1.377(5)
C7 - C8	1.388(5)	1.395(5)	1.395(4)	1.405(2)	1.393(4)	1.402(5)
C8 - C9	1.405(5)	1.394(4)	1.391(4)	1.387(2)	1.383(4)	1.383(4)
C9 - C10	1.385(6)	1.395(5)	1.382(4)	1.395(2)	1.395(4)	1.385(6)
C10 - C11	1.396(6)	1.394(5)	1.393(5)	1.404(2)	1.387(5)	1.397(6)
C11 - C12	1.383(5)	1.383(5)	1.381(4)	1.396(3)	1.385(4)	1.382(5)
C12 - C13	1.404(5)	1.393(4)	1.391(4)	1.395(2)	1.392(4)	1.391(5)
C13 - C14	1.402(5)	1.395(4)	1.392(4)	1.394(2)	1.389(4)	1.388(5)
C1 - C15	1.467(6)	1.467(5)	1.466(5)	1.470(3)	1.464(5)	1.460(6)
C6 - C15	1.476(5)	1.467(5)	1.476(4)	1.473(2)	1.468(4)	1.475(5)
C8 - C16	1.474(5)	1.471(5)	1.470(4)	1.472(2)	1.464(4)	1.463(5)
C13 - C16	1.469(5)	1.462(5)	1.463(5)	1.473(3)	1.460(5)	1.461(6)
C15 - O1	1.213(4)	1.212(4)	1.214(4)	1.215(2)	1.216(4)	1.223(4)
C16 - O2	1.217(5)	1.221(4)	1.214(4)	1.215(2)	1.223(4)	1.225(5)
C15 - C16	2.557(4)	2.543(4)	2.538(3)	2.539(3)	2.522(3)	2.525(4)

<sup>1</sup> From the multipolar refinement on high resolution data. These data are not directly comparable with those of the other refinements (all based on lower resolution data only), because the thermal motion is here better de-convoluted, giving in general slightly longer C-C distances for all bonds. For sake of homogeneity these data are not included in the plot 7. Anyway, the asymmetrical distribution of bonds follows the general trend observed at all pressures.

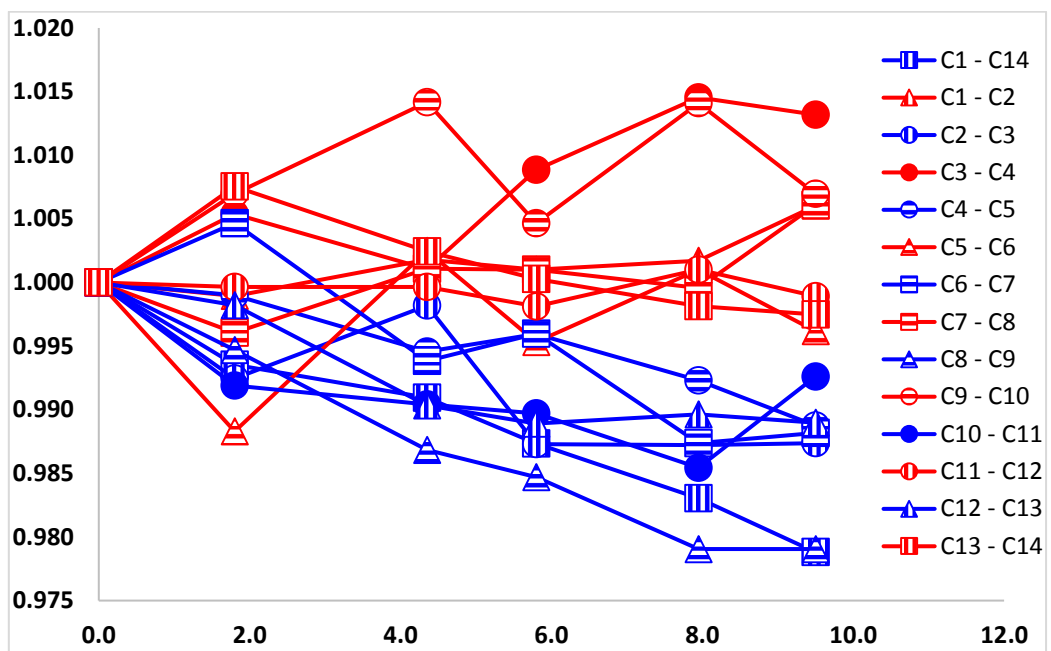


**Figure S1** Relative compression / expansion of C-C bonds as a function of pressure (in GPa) from experimental modelling. Distances are normalized to the value at ambient pressure and temperature. Blue and red symbols refer to the double bonds of the electronic configurations A and B respectively (Figure 1 in the main text).

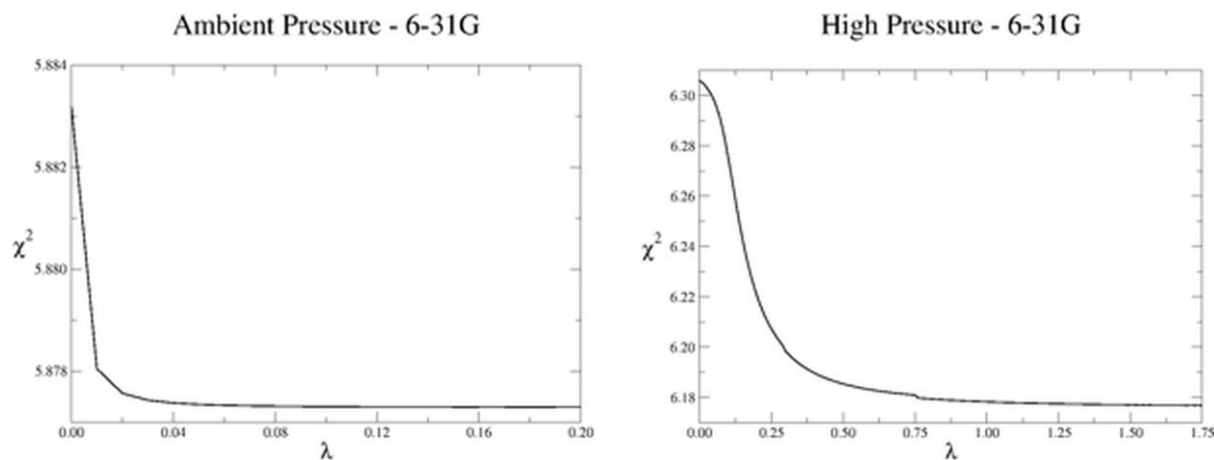


**Figure S2** Variation of the statistical agreement  $\chi^2$  in function of the external multiplier  $\lambda$  for the X-ray constrained ELMO-VB calculations performed at ambient and high pressures with the 6-31G basis-set.

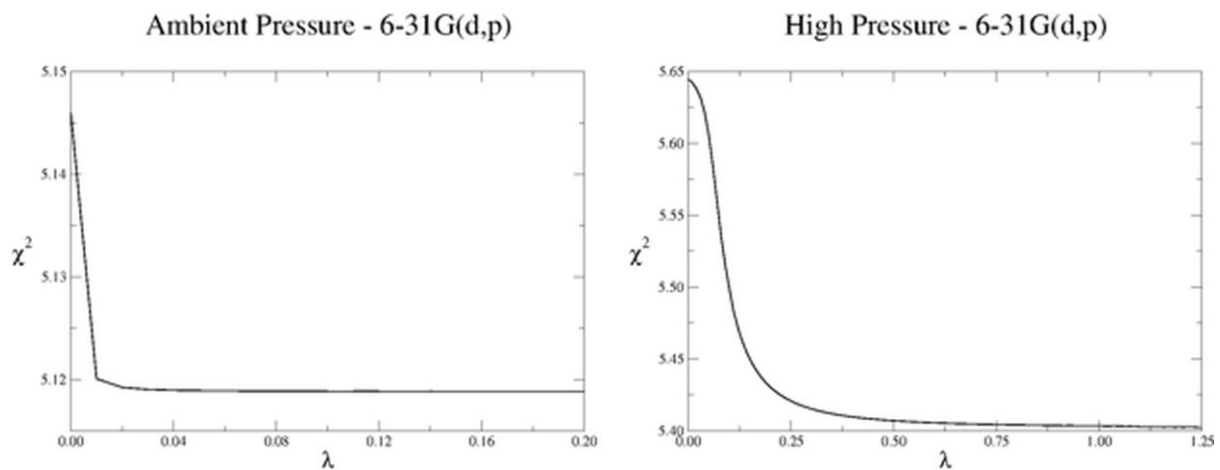


**Figure S3** Variation of the statistical agreement  $\chi^2$  in function of the external multiplier  $\lambda$  for the X-ray constrained ELMO-VB calculations performed at ambient and high pressures with the 6-31G(d,p) basis-set.

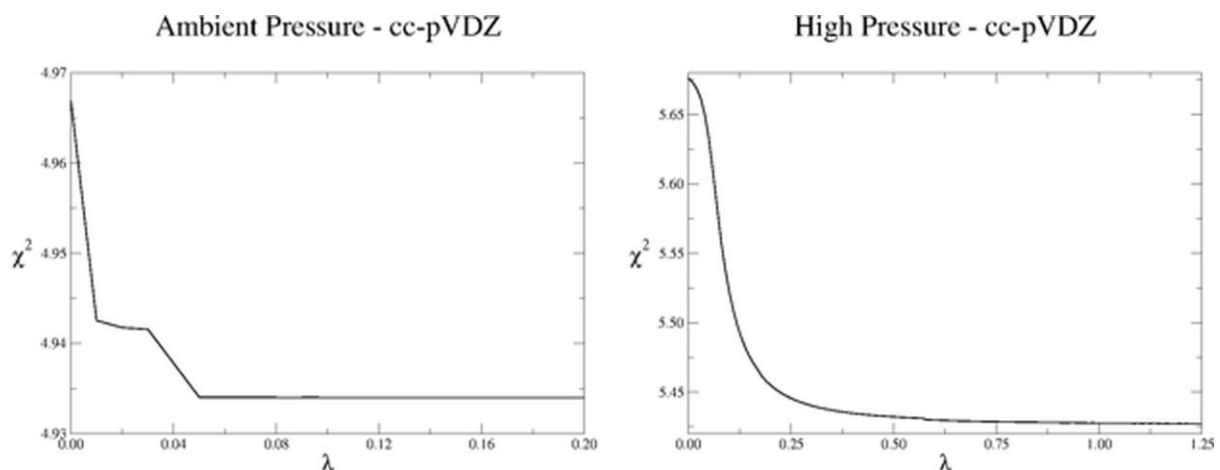


**Figure S4** Variation of the statistical agreement  $\chi^2$  in function of the external multiplier  $\lambda$  for the X-ray constrained ELMO-VB calculations performed at ambient and high pressures with the cc-pVDZ basis-set.

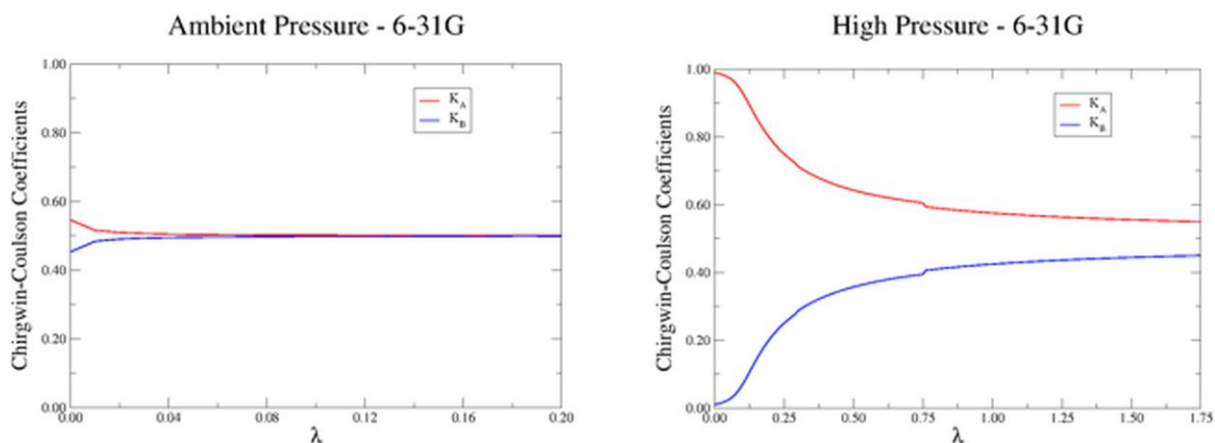


**Figure S5** Variation of the Chirgwin-Coulson coefficients in function of the external multiplier  $\lambda$  for the X-ray constrained ELMO-VB calculations performed at ambient and high pressures with the 6-31G basis-set.

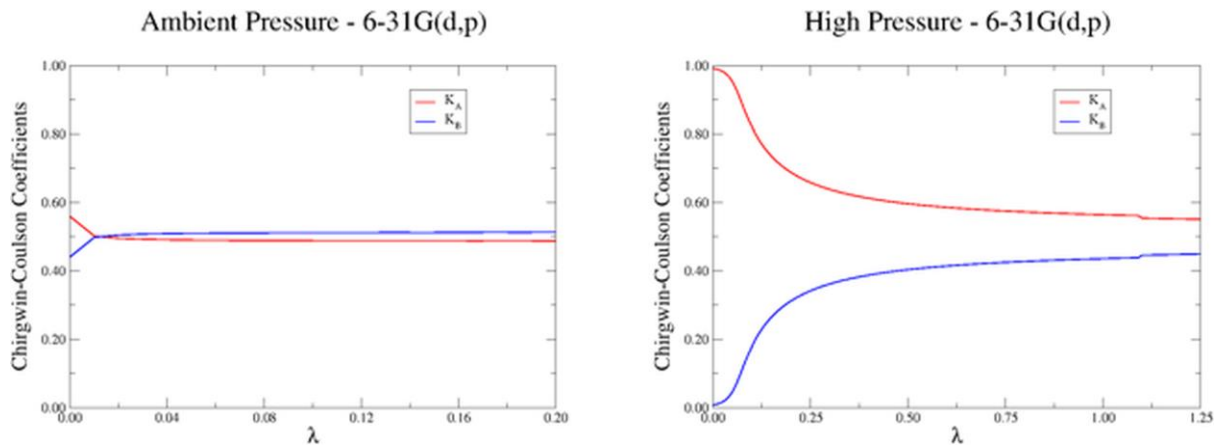


**Figure S6** Variation of the Chirgwin-Coulson coefficients in function of the external multiplier  $\lambda$  for the X-ray constrained ELMO-VB calculations performed at ambient and high pressures with the 6-31G(d,p) basis-set.

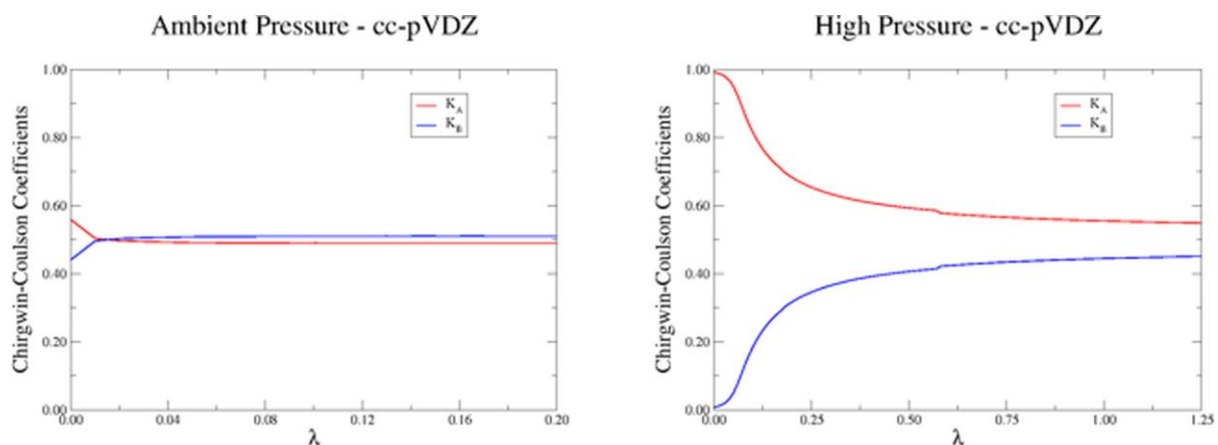


**Figure S7** Variation of the Chirgwin-Coulson coefficients in function of the external multiplier  $\lambda$  for the X-ray constrained ELMO-VB calculations performed at ambient and high pressures with the cc-pVDZ basis-set.